Cage Substitution Reactions of Monocarbollide Carbonyl Complexes of Iron: Generation of Iminium Groups at a Boron Vertex†

Andreas Franken, Shaowu Du, Paul A. Jelliss,‡ Jason A. Kautz, and F. Gordon A. Stone*

Department of Chemistry and Biochemistry, Baylor University, Waco, Texas 76798-7348

Received December 11, 2000

Treatment of $[N(PPh_3)_2][Fe(CO)_2(L)(\eta^5\text{-7-CB}_{10}H_{11})]$ (L = SMe_2, PPh_3) in SMe_2 or $O(CH_2)_4$ with H_2SO_4 yields the neutral charge-compensated complexes $[Fe(CO)_2(L)(\eta^5\text{-9-L}'\text{-7-CB}_{10}H_{10})]$ (L = SMe_2, L′ = SMe_2 (**2**), $O(CH_2)_4$ (**3**); L = PPh_3, L′ = SMe_2 (**4**), $O(CH_2)_4$ (**5**)). An X-ray crystallographic study of **2** established that one of the exopolyhedral SMe_2 groups is bonded to a boron in a β-site with respect to the carbon in the $\overline{CBBBB}$ ring coordinated to the iron atom. In contrast with these results, the salts $[N(PPh_3)_2][Fe(CO)_2(L)(\eta^5\text{-7-CB}_{10}H_{11})]$ (L = CO, PPh_3, $CNBu^t$) treated with NCMe and CF_3SO_3Me afford complexes $[Fe(CO)_2(L)(\eta^5\text{-9-}\{(E)\text{-N(Me)=C(H)Me}\}\text{-7-CB}_{10}H_{10})]$ (L = CO (**8**), PPh_3 (**9**), $CNBu^t$ (**10**)). An X-ray diffraction study on **8** established that the iminium group was attached to a β-B atom of the CB_4 iron-bonded ring. Compound **8** is readily hydrolyzed in the presence of a base catalyst affording $[Fe(CO)_3(\eta^5\text{-9-NH}_2\text{Me-7-CB}_{10}H_{10})]$ (**12**), and with $[Na][BH_3CN]$ yields $[Fe(CO)_3(\eta^5\text{-9-}\{\text{NH(Me)Et}\}\text{-7-CB}_{10}H_{10})]$ (**13**), the structure of which was determined by X-ray diffraction. The reaction between $[N(PPh_3)_2][Fe(CO)_3(\eta^5\text{-7-CB}_{10}H_{11})]$ and $Bu^tC{\equiv}CH$ gives $[N(PPh_3)_2][Fe(CO)_3\text{-}(\eta^2{:}\eta^5\text{-8-}\{(E)\text{-C(H)=C(H)Bu}^t\}\text{-7-CB}_{10}H_{10})]$ (**14**), which with NCMe in CF_3SO_3Me affords $[Fe(CO)_2(\eta^2{:}\eta^5\text{-8-}\{(E)\text{-C(H)=C(H)Bu}^t\}\text{-10-}\{(E)\text{-N(Me)=C(H)Me}\}\text{-7-CB}_{10}H_9)]$ (**16**). The site of attachment of the exopolyhedral iminium and *tert*-butylvinyl substituents to the cage was established by X-ray diffraction.

Introduction

In the anionic complexes $[Mo(CO)_4(\eta^5\text{-7-CB}_{10}H_{11})]^-$, $[Re(CO)_3(\eta^5\text{-7-CB}_{10}H_{11})]^{2-}$, and $[Fe(CO)_3(\eta^5\text{-7-CB}_{10}H_{11})]^-$ a transition metal ion is ligated both by carbonyl groups and a $[nido\text{-7-CB}_{10}H_{11}]^{3-}$ icosahedral cage fragment.[1] Their recent discovery allows detailed examination of a class of mononuclear metal compound which has been little studied previously.[2] Hitherto the only species of this type known were the molybdenum complexes $[Mo(CO)_3(L)(\eta^5\text{-7-OH-7-CB}_{10}H_{10})]^-$ (L = CO, PPh_3), which were obtained as unexpected products from reactions between $[Mo(CO)_6]$ and $[Na][nido\text{-B}_{10}H_{13}]$ and between $[Mo(CO)_3(NCMe)_2(PPh_3)]$ and $[NEt_4]_2[arachno\text{-B}_{10}H_{14}]$, respectively.[3] The chemistry of monocarbollide metal carbonyl complexes is potentially interesting. This is because there are electronic relationships with the ubiquitous cyclopentadienide metal carbonyl complexes, e.g., $[Fe(CO)_3(\eta^5\text{-7-CB}_{10}H_{11})]^-$ versus $[Fe(CO)_3(\eta^5\text{-C}_5H_5)]^+$, yet the cyclopentadienide and monocarbollide complexes display very different chemical behavior. The chief origin of this difference lies in the frequently adopted nonspectator role of the $[\eta^5\text{-7-CB}_{10}H_{11}]^{3-}$ ligand, a feature resulting in the formation of molecules with unusual structures and reactivities.[1]

In initial studies it was observed that the compound $[N(PPh_3)_2][Fe(CO)_3(\eta^5\text{-7-CB}_{10}H_{11})]$ (**1a**) reacted with donors (L) in the presence of hydride-abstracting reagents to yield zwitterionic complexes $[Fe(CO)_3(\eta^5\text{-9-L}'\text{-7-CB}_{10}H_{10})]$ (L′ = $O(CH_2)_4$, OEt_2, or SMe_2).[1c] In this paper we report a range of new ferracarborane zwitterionic molecules, isolating very unexpected products when acetonitrile is the substrate molecule.

Results and Discussion

It was anticipated that the reactivity of an $Fe(\eta^5\text{-7-CB}_{10}H_{11})$ fragment would likely be influenced by the donor−acceptor properties of the other ligands present. Accordingly, in addition to studies with **1a**, the complexes $[N(PPh_3)_2][Fe(CO)_2(L)(\eta^5\text{-7-CB}_{10}H_{11})]$ (L = PPh_3 (**1b**), $CNBu^t$ (**1c**), SMe_2 (**1d**), PMe_2Ph (**1e**)) were also employed. Compounds **1b** and **1c** were obtained from the reactions between **1a** and PPh_3 and $CNBu^t$, respectively, in THF (tetrahydrofuran) in the presence of Me_3NO.[1c] The related complexes **1d** and **1e** were similarly

† The compounds described in this paper have iron atoms incorporated into *closo*-1-carba-2-ferradodecaborane frameworks. To relate them to the many known iron species with η^5-coordinated cyclopentadienide ligands, for nomenclature purposes we treat the cages as *nido*-11-vertex ligands with numbering as for an icosahedron from which the 12th vertex has been removed.

‡ Current address: Department of Chemistry, Saint Louis University, St. Louis, MO 63103-2010.

(1) (a) Blandford, I.; Jeffery, J. C.; Jelliss, P. A.; Stone, F. G. A. *Organometallics* **1998**, *17*, 1402. (b) Jeffery, J. C.; Jelliss, P. A.; Rees, L. H.; Stone, F. G. A. *Organometallics* **1998**, *17*, 2258. (c) Ellis, D. D.; Franken, A.; Jelliss, P. A.; Stone, F. G. A.; Yu, P.-Y. *Organometallics* **2000**, *19*, 1993. (d) Ellis, D. D.; Franken, A.; Jelliss, P. A.; Kautz, J. A.; Stone, F. G. A. *J. Chem. Soc., Dalton Trans.* **2000**, 2509.

(2) Grimes, R. N. In *Comprehensive Organometallic Chemistry II*; Housecroft, C. E., Ed.; Pergamon: Oxford, 1995; Section 9 in Vol. 1

10.1021/om001057x CCC: $20.00
Publication on Web 03/23/2001

Table 1. Analytical and Physical Data

compd[a]	yield/%	$\nu_{max}(CO)^b$/cm^{-1}	anal./%[c] C	H	N
$[N(PPh_3)_2][Fe(CO)_2(SMe_2)(\eta^5\text{-}7\text{-}CB_{10}H_{11})]$ (**1d**)	81	1993s, 1940s	58.4 (58.3)	5.5 (5.6)	1.7 (1.7)
$[N(PPh_3)_2][Fe(CO)_2(PMe_2Ph)(\eta^5\text{-}7\text{-}CB_{10}H_{11})]$ (**1e**)	72	1988s, 1934s	60.9 (61.4)	5.8 (5.7)	1.5 (1.5)
$[Fe(CO)_2(SMe_2)(\eta^5\text{-}9\text{-}SMe_2\text{-}7\text{-}CB_{10}H_{10})]$ (**2**)	56	2011s, 1964s	23.6 (23.0)	5.6 (6.1)	
$[Fe(CO)_2(SMe_2)(\eta^5\text{-}9\text{-}O(CH_2)_4\text{-}7\text{-}CB_{10}H_{10})]$ (**3**)	79	2009s, 1956s	28.5 (28.7)	6.7 (6.4)	
$[Fe(CO)_2(PPh_3)(\eta^5\text{-}9\text{-}SMe_2\text{-}7\text{-}CB_{10}H_{10})]$ (**4**)	76	2009s, 1959s	48.3 (48.8)	5.6 (5.5)	
$[Fe(CO)_2(PPh_3)(\eta^5\text{-}9\text{-}O(CH_2)_4\text{-}7\text{-}CB_{10}H_{10})]$ (**5**)	82	2005s, 1953s	51.8 (52.1)	5.9 (5.8)	
$[Fe(CO)_2(PPh_3)(\eta^5\text{-}9\text{-}NCBu^t\text{-}7\text{-}CB_{10}H_{10})]$ (**6**)	62	2009s, 1958s	52.4 (53.2)	6.0 (5.8)	2.5 (2.4)
$[Fe(CO)_2(PMe_2Ph)(\eta^5\text{-}9\text{-}NCMe\text{-}7\text{-}CB_{10}H_{10})]$ (**7**)	24	2007s, 1957s	36.9 (37.1)	5.7 (5.7)	3.2 (3.3)
$[Fe(CO)_3(\eta^5\text{-}9\text{-}\{(E)\text{-}N(Me){=}C(H)Me\}\text{-}7\text{-}CB_{10}H_{10})]$ (**8**)	42	2076s, 2029m, 2011m	25.7 (25.7)	5.3 (5.2)	4.2 (4.3)
$[Fe(CO)_2(PPh_3)(\eta^5\text{-}9\text{-}\{(E)\text{-}N(Me){=}C(H)Me\}\text{-}7\text{-}CB_{10}H_{10})]$ (**9**)	87	2005s, 1953s	49.7 (48.7)	5.7 (5.5)	2.4 (2.3)[d]
$[Fe(CO)_2(CNBu^t)(\eta^5\text{-}9\text{-}\{(E)\text{-}N(Me){=}C(H)Me\}\text{-}7\text{-}CB_{10}H_{10})]$ (**10**)	83	2023s, 1982s[e]	34.4 (34.6)	6.8 (6.9)	7.3 (7.4)
$[Fe(CO)_2(PMe_2Ph)(\eta^5\text{-}9\text{-}\{(E)\text{-}N(H){=}C(H)Me\}\text{-}7\text{-}CB_{10}H_{10})]$ (**11**)	43	2005s, 1952s	37.1 (36.9)	6.2 (6.2)	3.2 (3.3)
$[Fe(CO)_3(\eta^5\text{-}9\text{-}NH_2Me\text{-}7\text{-}CB_{10}H_{10})]$ (**12**)	88	2078s, 2029m, 2005m	20.4 (19.9)	5.1 (5.0)	4.8 (4.7)
$[Fe(CO)_3(\eta^5\text{-}9\text{-}\{NH(Me)Et\}\text{-}7\text{-}CB_{10}H_{10})]$ (**13**)	86	2078s, 2028m, 2009m	26.0 (25.5)	5.7 (5.8)	4.2 (4.3)
$[N(PPh_3)_2][Fe(CO)_2(\eta^2{:}\eta^5\text{-}8\text{-}\{(E)\text{-}C(H){=}C(H)Bu^t\}\text{-}7\text{-}CB_{10}H_{10})]$ (**14**)[f]	45	2003s, 1954s			
$[N(PPh_3)_2][Fe(CO)_2(PPh_3)(\eta^5\text{-}8\text{-}\{(E)\text{-}C(H){=}C(H)Bu^t\}\text{-}7\text{-}CB_{10}H_{10})]$ (**15**)	44	1992s, 1941s	66.8 (67.2)	6.0 (5.9)	1.2 (1.3)
$[Fe(CO)_2(\eta^2{:}\eta^5\text{-}8\text{-}\{(E)\text{-}C(H){=}C(H)Bu^t\}\text{-}10\text{-}\{(E)\text{-}N(Me){=}C(H)Me\}\text{-}7\text{-}CB_{10}H_9)]$ (**16**)	42	2017s, 1964s	38.1 (37.8)	7.1 (7.1)	3.5 (3.7)

[a] All compounds are yellow except **15** and **16** (orange). [b] Measured in CH_2Cl_2; medium-intensity bands observed at ca. 2550 cm^{-1} in the spectra of all compounds are due to B−H absorptions. [c] Calculated values are given in parentheses. Where analytically pure products were not isolated, mass spectral data are given. [d] Contains 0.5 molar equiv CH_2Cl_2, as confirmed in an ^{1}H NMR spectrum. EI mass spectrum: *m/z* 505.23 ([**10** − 2 CO]$^+$) (calc 505.43). [e] $\nu_{max}(NC)$ = 2177m cm^{-1}. [f] EI mass spectrum: *m/z* 324.96 ([**14**]$^+$) (calc 325.22).

Chart 1

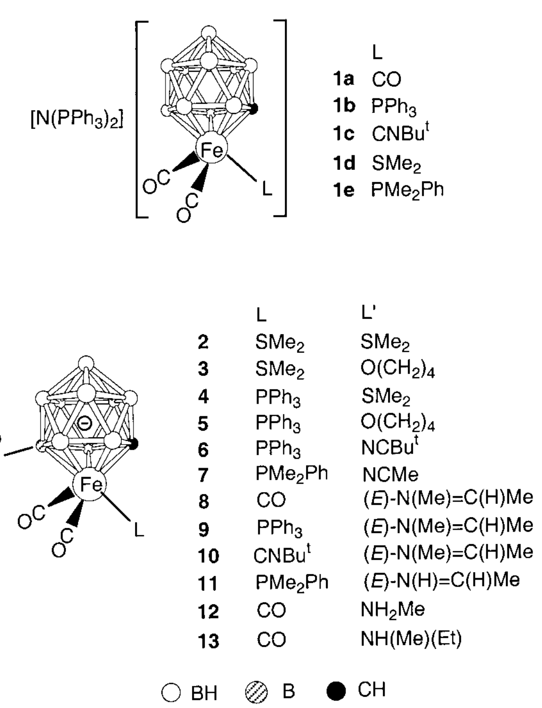

prepared from SMe_2 and PMe_2Ph and were characterized by the data given in Tables 1−3.

Like its parent compound **1a**, when the salt **1d** is dissolved in SMe_2 or THF and the mixture treated with concentrated H_2SO_4, the charge-compensated molecules $[Fe(CO)_2(SMe_2)(\eta^5\text{-}9\text{-}L'\text{-}7\text{-}CB_{10}H_{10})]$ (L′ = SMe_2 (**2**), $O(CH_2)_4$ (**3**)), respectively, are formed. Similarly, complex **1b** in CH_2Cl_2 together with SMe_2 or THF in the presence of CF_3SO_3H yielded the species $[Fe(CO)_2(PPh_3)(\eta^5\text{-}9\text{-}L'\text{-}7\text{-}CB_{10}H_{10})]$ (L′ = SMe_2 (**4**), $O(CH_2)_4$ (**5**)), respectively. Data characterizing the complexes **2**−**5** are given in Tables 1−3. Isomers are possible according to whether the donor molecule is bonded to a boron vertex located at an α- or β-site with respect to the carbon in

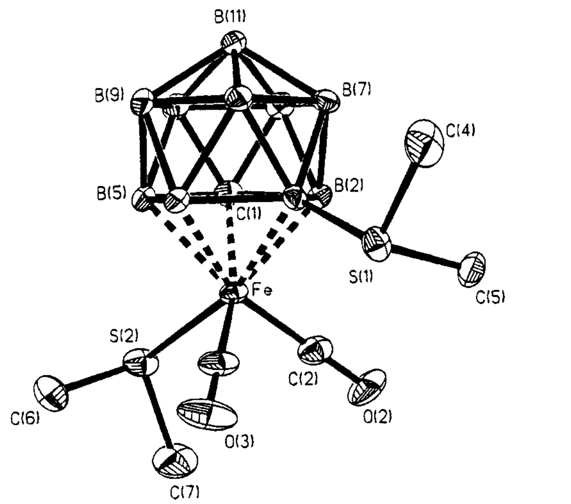

Figure 1. Structure of $[Fe(CO)_2(SMe_2)(\eta^5\text{-}9\text{-}SMe_2\text{-}7\text{-}CB_{10}H_{10})]$ (**2**), showing the crystallographic labeling scheme. Hydrogen atoms are omitted for clarity, and thermal ellipsoids are shown at the 40% probability level.

the $\overline{\text{CBBBB}}$ pentagonal ring coordinated to the iron atom. However, there was no evidence from their NMR spectra for the formation of more than one isomer. In the molecule $[Fe(CO)_3(\eta^5\text{-}9\text{-}O(CH_2)_4\text{-}7\text{-}CB_{10}H_{10})]$, isolated in the initial study of **1a**,[1c] X-ray diffraction revealed the THF group was attached to one of the β-boron atoms in the $\overline{\text{CB}\textit{BB}\text{B}}$ ring. From this it seemed likely that the same regiochemistry would prevail in the new species. To confirm this, an X-ray diffraction study was made on **2**. Selected structural parameters are given in Table 4, and the molecule is shown in Figure 1.

It is immediately apparent that the cage SMe_2 group is attached to a boron atom situated in a β-site with respect to the carbon in the iron-ligating $\overline{\text{CB}\textit{BB}\text{B}}$ ring. This indicates that within the cage it is the hydrogens of the β-BH vertexes that are the most susceptible to

Table 2. ^{1}H and ^{13}C NMR Data[a]

	^{1}H/δ[b]	^{13}C/δ[c]
1d	1.83 (br s, 1 H, cage CH), 2.37 (s, 6 H, Me), 7.47−7.66 (m, 30 H, Ph)	215.2 (CO), 134.0−126.7 (Ph), 49.7 (br, cage CH), 26.8 (Me)
1e	1.02 (br s, 1 H, cage CH), 1.85 (d, 6 H, PMe, *J*(PH) = 8), 7.36−7.67 (m, 35 H, Ph)	215.1 (d, CO, *J*(PC) = 24), 138.1−126.7 (Ph), 48.5 (br, cage CH), 17.9 (d, Me, *J*(PC) = 34)
2	1.75 (br s, 1 H, cage CH), 2.34, 2.42 (s × 2, 6 H, Me), 2.48 (br s, 6 H, Me)	213.6 (CO), 211.8 (CO), 49.2 (br, cage CH), 26.5 (SMe), 26.0 (SMe), 25.7 (SMe)
3	1.57 (br s, 1 H, cage CH), 2.11 (m, 4 H, CH$_2$), 2.42 (s, 6 H, Me), 4.23 (m, 4 H, OCH$_2$)	214.2 (CO), 212.0 (CO), 80.6 (OCH$_2$), 47.1 (br cage CH), 26.5 (SMe), 25.2 (CH$_2$)
4	0.38 (br s, 1 H, cage CH), 2.63, 2.53 (s × 2, 6 H, Me), 7.53−7.67 (m, 15 H, Ph)	215.7 (d, CO, *J*(PC) = 29), 211.7 (d, CO, *J*(PC) = 23), 134.2−128.8 (Ph), 52.9 (br, cage CH), 26.4 (SMe), 25.7 (SMe)
5	0.21 (br s, 1 H, cage CH), 3.25 (m, 4 H, CH$_2$), 4.43 (m, 4 H, OCH$_2$), 7.44 − 7.63 (m, 15 H, Ph)	216.2 (d, CO, *J*(PC) = 27), 212.0 (d, CO, *J*(PC) = 23), 133.9−128.6 (Ph), 80.8 (OCH$_2$), 48.7 (br, cage CH), 25.3 (CH$_2$)
6	0.28 (br s, 1 H, cage CH), 1.54 (s, 9 H, Bu^t), 7.44−7.67 (m, 15 H, Ph)	216.3 (d, CO, *J*(PC) = 28), 211.1 (d, CO, *J*(PC) = 22), 133.9−128.3 (Ph), 119.6 (NC), 60.6 (*C*Me$_3$), 51.5 (br, cage CH), 27.0 (C*Me$_3$*)
7	0.85 (br s, 1 H, cage CH), 1.94 (d, 3 H, PMe, *J*(PH) = 9), 1.98 (d, 3 H, PMe, *J*(PH) = 9), 2.58 (s, 3 H, Me), 7.45−7.57 (m, 5 H, Ph)	213.8 (d, CO, *J*(PC) = 29), 211.8 (d, CO, *J*(PC) = 24), 136.2−128.8 (Ph), 113.0 (NC), 47.5 (br, cage CH), 4.2 (Me)
8	1.83 (br s, 1 H, cage CH), 2.56 (d, 3 H, C(H)*Me*, *J*(HH) = 6), 3.64 (s, 3 H, Me), 7.97 (vbr s, 1 H, =CH)	207.0 (CO), 179.0 (C=N), 53.6 (NMe), 48.0 (br, cage CH), 21.1 (C(H)*Me*)
9	0.35 (br s, 1 H, cage CH), 2.65 (s, 3 H, C(H)*Me*), 3.72 (s, 3 H, NMe), 7.45−7.63 (m, 15 H, Ph), 7.95 (br s, 1 H, =CH)	215.9 (d, CO, *J*(PC) = 28), 212.0 (d, CO, *J*(PC) = 24), 177.1 (C=N), 133.9−128.6 (Ph), 53.6 (NMe), 50.1 (br, cage CH), 21.1 (C(H)*Me*)
10	1.49 (s, 9 H, Bu^t), 1.61 (br s, 1 H, cage CH), 2.53 (s, 3 H, C(H)*Me*), 3.59 (s, 3 H, NMe), 7.88 (br s, 1 H, =CH)	211.5 (CO), 211.0 (CO), 176.8 (C=N), 152.0 (*C*NBu^t), 59.0 (*C*Me$_3$), 53.4 (NMe), 46.5 (br, cage CH), 30.3 (C*Me$_3$*), 20.9 (C(H)*Me*)
11	1.30 (br s, 1 H, cage CH), 1.92 (d, 3 H, PMe, *J*(PH) = 10), 1.96 (d, 3 H, PMe, *J*(PH) = 9), 2.22 (d, 3 H, C(H)*Me*, *J*(HH) = 5), 7.46−7.57 (m, 5 H, Ph), 7.84 (dq, 1 H, =CH, *J*(HH) = 5, 20), 9.10 (d br, 1 H, NH, *J*(HH) = 20)	214.3 (d, CO, *J*(PC) = 29), 212.4 (d, CO, *J*(PC) = 24), 176.1 (C=N), 136.6−128.8 (Ph), 47.5 (br, cage CH), 23.2 (C(H)*Me*), 18.5 (d, Me, *J*(PC) = 34), 16.6 (d, Me, *J*(PC) = 36)
12	1.85 (br s, 1 H, cage CH), 2.72 (s, 3 H, NMe), 4.54 (br m, 1 H, NH), 4.60 (br m, 1 H, NH)	207.0 (CO), 48.8 (br, cage CH), 34.4 (NMe)
13	1.30 (m, 6 H, CH$_2$*Me*), 1.87 (br s, 2 H, cage CH), 2.66, 2.76 (m × 2, 8 H, NMe + CH$_2$), 3.35, 3.48 (m × 2, 2 H, CH$_2$), 3.97 (br m, 2 H, NH)	207.1 (CO), 52.7, 52.5 (CH$_2$), 48.9 (br, cage CH), 40.5, 40.3 (NMe), 12.7, 12.6 (*Me*, CH$_2$*Me*)
14	0.62 (br s, 1 H, cage CH), 1.02 (s, 9 H, Bu^t), 4.29 (d, 1 H, (C(*H*)Bu^t), *J*(HH) = 11), 4.72 (d, 1 H, BCH, *J*(HH) = 11), 7.48 − 7.67 (m, 30 H, Ph)	217.1 (CO), 211.5 (CO), 134.0−126.7 (Ph), 100.6 (*C*(H)Bu^t), 82.0 (br, C(H)B), 58.4 (*C*Me$_3$), 47.2 (br, cage CH), 33.7 (C*Me$_3$*)
15	0.49 (br s, 1 H, cage CH), 1.12 (s, 9 H, Bu^t), 5.34 (d, 1 H, C(*H*)Bu^t, *J*(HH) = 18), 5.35 (d, 1 H, C(H)B, *J*(HH) = 18), 7.36 − 7.65 (m, 45 H, Ph)	217.9 (d, CO, *J*(PC) = 23), 213.4 (d, CO, *J*(PC) = 23), 141.9 (*C*(H)Bu^t), 135.8−126.7 (Ph), 82.0 (br, C(H)B), 66.1 (*C*Me$_3$), 55.9 (br, cage CH), 31.3 (C*Me$_3$*)
16	0.08 (br s, 1 H, cage CH), 1.22 (s, 9 H, Bu^t), 2.54 (d, 3 H, C(H)*Me*, *J*(HH) = 6), 3.61 (s, 3 H, NMe), 3.80 (d, 1 H, C(*H*)Bu^t, *J*(HH) = 14), 4.77 (d, 1 H, C(H)B, *J*(HH) = 14), 7.88 (br s, 1 H, C(*H*)Me)	213.0 (CO), 210.4 (CO), 177.5 (C=N), 111.4 (*C*(H)Bu^t), 85.0 (br, BCH), 65.9 (*C*Me$_3$), 53.8 (NMe), 44.6 (br, cage CH), 31.0 (C*Me$_3$*), 20.9 (C(H)*Me*)

[a] Chemical shifts (δ) in ppm, coupling constants (*J*) in hertz, measurements at ambient temperatures in CD$_2$Cl$_2$. [b] Resonances for terminal BH protons occur as broad unresolved signals in the range δ ca. −1 to 3. [c] ^{1}H-decoupled chemical shifts are positive to high frequency of SiMe$_4$.

removal by electrophiles and are therefore likely to be the most hydridic. The B(3)−S(1) distance of 1.921(4) Å is perceptibly longer than those in *nido*-9-SMe$_2$-7,8-C$_2$B$_9$H$_{11}$ (1.884(3) Å)[4a] and similar molecules.[4b] The iron-coordinated SMe$_2$ group (Fe−S = 2.2842(9) Å) in **2** lies transoid to B(3) (S(2)−Fe−B(3) = 162.67(11)°), while the Me groups attached to S(1) point away from the Fe(CO)$_2$SMe$_2$ moiety. This arrangement presumably serves to reduce steric crowding.

Establishment of the molecular structure of **2** allows ready interpretation of the NMR data (Tables 2 and 3) for this species and also those of complexes **3**−**5**. In the ^{11}B{^{1}H} NMR spectra of all the complexes one resonance remained a singlet when a fully coupled ^{11}B spectrum was measured (Table 3), and this signal may therefore be attributed to the boron nucleus of the BL′ group. In all the ^{13}C{^{1}H} NMR spectra there are two resonances for the nonequivalent CO groups, in agreement with the asymmetry of the molecules, an unavoidable consequence of substitution at a single β-boron vertex in the CB*BB*B coordinating face of the carborane cage. A diagnostic broad peak is seen in each spectrum for the cage CH group (δ 47.1−52.9). Corresponding signals in the ^{1}H NMR spectra occur at δ 1.75 and 1.57 for complexes **2** and **3** but further upfield at δ 0.38 and 0.21 for compounds **4** and **5**, no doubt because of the superior donor capacity of the ligand PMe$_2$Ph compared with SMe$_2$. This results in a downfield shift of these signals, although it is noted that this effect does not manifest itself in the corresponding ^{13}C{^{1}H} chemical shifts. Evidently in solution the Me substituents of one of the two SMe$_2$ groups in **2** do not undergo inversion at the S atom on the NMR time scale since in the ^{1}H and ^{13}C{^{1}H} NMR spectra there are three signals: ^{1}H, δ 2.34, 2.42, and 2.48 (rel int 3:3:6); ^{13}C{^{1}H}, δ 26.5, 26.0, and 25.7. The molecules **4** and [Fe(CO)$_3$(η^5-9-SMe$_2$-7-CB$_{10}$H$_{10}$)] have no iron-ligating SMe$_2$ groups, yet each displays in

(3) (a) Wegner, P. A.; Guggenberger, L. J.; Muetterties, E. L. *J. Am. Chem. Soc.* **1970**, *92*, 3473. (b) Fontaine, X. L. R.; Greenwood, N. N.; Kennedy, J. D.; MacKinnon, P. I.; Macpherson. I. *J. Chem. Soc., Dalton Trans.* **1987**, 2385.

(4) (a) Cowie, J.; Hamilton, E. J. M.; Laurie, J. C. V.; Welch, A. J. *Acta Crystallogr.* **1986**, *C44*, 1648. (b) Stíbr, B. *Chem. Rev.* **1992**, *92*, 225.

Table 3. ^{11}B and ^{31}P NMR Data[a]

	$^{11}B\{^1H\}/\delta^b$	$^{31}P\{^1H\}/\delta^c$
1d	5.3 (1 B), −4.4 (2 B), −5.5 (2 B), −7.8 (1 B), −13.1 (2 B), −17.4 (2 B)	21.7
1e	6.1 (1 B), −2,9 (2 B), −6.4 (2 B), −8.5 (1 B), −12.7 (2 B), −17.7 (2 B)	35.3 ($Fe(PMe_2Ph)$), 21.7 ($N(PPh_3)_2$)
2	5.9 (1 B), −1.5 (1 B), *−2.7 (1 B), −3.5 (1 B), −6.5 (1 B), −9.6 (1 B), −13.1 (1 B), −15.1 (2 B), −17.7 (1 B)	
3	*17.4 (1 B), 3.3 (1 B), −4.8 (2 B), −8.9 (2 B), −14.3 (2 B), −18.4 (1 B), −20.4 (1 B)	
4	7.0 (1 B), *−0.5 (1 B), −0.6 (1 B), −5.2 (1 B), −6.4 (1 B), −10.0 (1 B), −12.6 (1 B), −14.9 (1 B), −16.2 (1 B), −17.5 (1 B)	66.8
5	*18.4 (1 B), 4.7 (1 B), −3.1 (1 B), −6.9 (1 B), −8.3 (1 B), −9.5 (1 B), −13.4 (1 B), −14.2 (1 B), −18.8 (1 B), −20.7 (1 B)	65.7
6	5.8 (2 B), −1.4 (1 B), *−4.1 (1 B), −5.9 (1 B), −8.1 (1 B), −12.7 (2 B), −17.5 (2 B)	66.1, 65.2[d]
7	4.7 (1 B), *−2.7 (1 B), −3.2 (1 B), −6.0 (1 B), −7.2 (1 B), −8.5 (1 B), −12.7 (2 B), −17.6 (2 B)	33.7
8	10.2 (1 B), *8.3 (1 B), −1.6 (1 B), −5.8 (2 B), −7.4 (1 B), −9.6 (1 B), −10.1 (1 B), −15.8 (2 B)	
9	*5.6 (1 B), 5.4 (1 B), −2.2 (1 B), −5.8 (2 B), −8.7 (1 B), −12.1 (1 B), −12.7 (1 B), −17.3 (2 B)	65.8
10	*6.1 (1 B), 5.4 (1 B), −3.1 (1 B), −6.8 (2 B), −8.5 (1 B), −12.1 (2 B), −17.4 (2 B)	
11	*5.8 (1 B), 5.4 (1 B), −4.1 (1 B), −5.9 (1 B), −8.2 (2 B), −13.2 (2 B), −18.0 (2 B)	33.3
12	11.0 (1 B), *9.2 (1 B), −1.2 (1 B), −6.3 (2 B), −7.4 (1 B), −10.4 (2 B), −17.0 (2 B)	
13	*12.6 (1 B), 11.2 (1 B), −0.6 (1 B), −6.7 (3 B), −9.6 (1 B), −10.0 (1 B), −16.7 (1 B), −17.6 (1 B)	
14	*12.6 (1 B), 7.2 (1 B), 4.8 (1 B), −3.0 (2 B), −5.7 (1 B), −13.8 (1 B), −17.0 (1 B), −18.1 (1 B), −20.8 (1 B)	
15	6.4 (1 B), *2.4 (1 B), −1.4 (1 B), −2.5 (1 B), −6.4 (1 B), −7.7 (1 B), −9.5 (1 B), −14.7 (2 B), −17.2 (1 B)	66.8 ($Fe(PPh_3)$), 21.7 ($N(PPh_3)_3$)
16	*9.5 (1 B), *3.6 (1 B), 3.5 (2 B), −3.2 (2 B), −13.5 (1 B), −17.7 (1 B), −18.9 (1 B), −20.1 (1 B)	

[a] Chemical shifts (δ) in ppm, coupling constants (J) in hertz, measurements at ambient temperatures in CD_2Cl_2. [b] Chemical shifts (δ) are positive to high frequency of $BF_3\cdot Et_2O$ (external). Signals ascribed to more than one boron nucleus may result from overlapping peaks and do not necessarily indicate symmetry equivalence. Peaks marked with an asterisk are assigned to cage-boron nuclei carrying L substituents (see text), since they occur as singlets in fully coupled ^{11}B spectra. [c] $^{31}P\{^1H\}$ chemical shifts (δ) are positive to high frequency of H_3PO_4 (external). [d] Weak signal, see text.

Table 4. Selected Internuclear Distances (Å) and Angles (deg) for [Fe(CO)$_2$(SMe$_2$)(η^5-9-SMe$_2$-7-CB$_{10}$H$_{10}$)] (2)

Fe−C(3)	1.757(4)	Fe−C(2)	1.780(4)	Fe−C(1)	2.132(3)	Fe−B(3)	2.140(4)
Fe−B(5)	2.142(4)	Fe−B(2)	2.145(4)	Fe−B(4)	2.183(4)	Fe−S(2)	2.2842(9)
B(3)−S(1)	1.921(4)	C(2)−O(2)	1.148(4)	C(3)−O(3)	1.141(4)	S(1)−C(4)	1.793(4)
S(1)−C(5)	1.796(4)	S(2)−C(7)	1.802(4)	S(2)−C(6)	1.807(4)		

C(3)−Fe−C(2)	92.7(2)	C(3)−Fe−C(1)	162.5(2)	C(2)−Fe−C(1)	104.2(2)
C(3)−Fe−B(3)	90.9(2)	C(2)−Fe−B(3)	104.6(2)	C(3)−Fe−B(5)	116.8(2)
C(2)−Fe−B(5)	149.7(2)	C(3)−Fe−B(2)	134.5(2)	C(2)−Fe−B(2)	79.8(2)
C(3)−Fe−B(4)	80.8(2)	C(2)−Fe−B(4)	152.5(2)	C(3)−Fe−S(2)	91.00(12)
C(2)−Fe−S(2)	92.54(12)	C(1)−Fe−S(2)	92.83(9)	B(3)−Fe−S(2)	162.67(11)
B(5)−Fe−S(2)	81.00(11)	B(2)−Fe−S(2)	133.76(11)	B(4)−Fe−S(2)	114.15(10)
S(1)−B(3)−Fe	113.4(2)	S(1)−B(3)−B(2)	123.0(2)	S(1)−B(3)−B(4)	121.4(2)
O(2)−C(2)−Fe	176.4(3)	O(3)−C(3)−Fe	179.7(4)	C(4)−S(1)−C(5)	99.7(2)
C(4)−S(1)−B(3)	106.6(2)	C(5)−S(1)−B(3)	104.1(2)	C(7)−S(2)−C(6)	98.3(2)
C(7)−S(2)−Fe	111.3(2)	C(6)−S(2)−Fe	108.23(14)		

their ^{1}H and $^{13}C\{^1H\}$ NMR spectra a pair of Me resonances. For **4** these peaks are seen at δ 2.63 and 2.53 (^{1}H) and at δ 26.4 and 25.7 ($^{13}C\{^1H\}$), while for [Fe(CO)$_3$(η^5-9-SMe$_2$-7-CB$_{10}$H$_{10}$)][1c] they occur at δ 2.53 and 2.42 (^{1}H) and at δ 26.4 and 25.7 ($^{13}C\{^1H\}$). From these results it may be inferred that in all three molecules it is the Me groups of the BSMe$_2$ fragments that do not invert at the S atom in solution at ambient temperatures.

It was observed qualitatively that the syntheses proceeded more readily with **1b** than with **1a** presumably because replacement of a CO group on iron by the better donor PPh$_3$ enhances electron density in the cage. Thus hydrogen atoms at the β-B sites are rendered increasingly hydridic and so more easily abstracted by a strong electrophile. Reaction between **1b** and NCBu^t, and employing in this instance CF_3SO_3Me as the hydride removal reagent, also yielded a zwitterionic molecule, [Fe(CO)$_2$(PPh$_3$)(η^5-9-NCBu^t-7-CB$_{10}$H$_{10}$)] (**6**). A similar reaction occurs using CF_3SO_3H, but the process proceeds less cleanly. The $^{31}P\{^1H\}$ NMR spectrum of **6** displayed a resonance at δ 66.1, but there was also a much weaker signal at δ 65.2, providing somewhat tenuous evidence for the presence of a second isomer. However the presence of this species could not be detected in the ^{1}H or $^{13}C\{^1H\}$ NMR spectra.

It is assumed that in the syntheses of **2**−**6** nucleophilic substitution is facilitated by removal of H$^-$ from a β-BH vertex by H$^+$ or Me$^+$ with release of H_2 or CH_4, although no attempt was made to identify these species. This step would generate a site on the cage for nucleophilic attack by any donor present, a process first observed by Hawthorne and co-workers[5] in related chemistry where treatment of the dianion [Fe(η^5-7,8-C$_2$B$_9$H$_{11}$)$_2$]$^{2-}$ with concentrated acid followed by addition of a dialkyl sulfide afforded the monoanionic species [Fe(η^5-7,8-C$_2$B$_9$H$_{11}$)(η^5-10-SR$_2$-7,8-C$_2$B$_9$H$_{10}$)]$^-$. Related to this is the synthesis of *nido*-8-SMe$_2$-7-CB$_{10}$H$_{12}$ by treating [NMe$_4$][*nido*-7-CB$_{10}$H$_{13}$] and SMe$_2$ with sulfuric

(5) Hawthorne, M. F.; Warren, L. F.; Callahan, K. P.; Travers, N. F. *J. Am. Chem. Soc.* **1971**, *93*, 2407.

Table 5. Selected Internuclear Distances (Å) and Angles (deg) for $[Fe(CO)_3(\eta^5\text{-}9\text{-}\{(E)\text{-}N(Me){=}C(H)Me\}\text{-}7\text{-}CB_{10}H_{10})]$ (8)

Fe−C(4)	1.790(3)	Fe−C(3)	1.800(3)	Fe−C(2)	1.813(3)	Fe−B(5)	2.144(3)
Fe−C(1)	2.150(3)	Fe−B(2)	2.185(3)	Fe−B(4)	2.188(3)	Fe−B(3)	2.199(3)
B(3)−N	1.562(6)	B(3)−N(1A)	1.67(2)	C(2)−O(2)	1.142(4)	C(3)−O(3)	1.142(4)
C(4)−O(4)	1.145(4)	N−C(5)	1.301(10)	N−C(7)	1.504(12)	C(5)−C(6)	1.46(2)
N(1A)-C(5A)	1.25(3)	N(1A)-C(7A)	1.59(4)	C(5A)-C(6A)	1.46(4)		

C(4)−Fe−C(3)	96.35(14)	C(4)−Fe−C(2)	91.04(14)	C(3)−Fe−C(2)	90.46(14)
C(4)−Fe−B(5)	166.46(12)	C(3)−Fe−B(5)	95.38(13)	C(2)−Fe−B(5)	95.61(13)
C(4)−Fe−C(1)	122.44(13)	C(3)−Fe−C(1)	140.68(13)	C(2)−Fe−C(1)	83.27(12)
C(4)−Fe−B(2)	83.91(12)	C(3)−Fe−B(2)	158.14(13)	C(2)−Fe−B(2)	111.40(13)
C(4)−Fe−B(4)	128.00(13)	C(3)−Fe−B(4)	77.82(13)	C(2)−Fe−B(4)	139.90(14)
C(4)−Fe−B(3)	86.84(12)	C(3)−Fe−B(3)	108.28(13)	C(2)−Fe−B(3)	161.26(13)
N−B(3)−B(4)	116.7(3)	N(1A)−B(3)−B(4)	140.5(6)	N−B(3)−B(2)	131.9(3)
N(1A)−B(3)−B(2)	109.6(6)	N−B(3)−Fe	117.1(2)	N(1A)−B(3)−Fe	119.5(4)
O(2)−C(2)−Fe	179.4(3)	O(3)−C(3)−Fe	178.0(3)	O(4)−C(4)−Fe	179.7(3)
C(5)−N−C(7)	115.8(6)	C(5)−N−B(3)	125.8(5)	C(7)−N−B(3)	118.4(6)
N−C(5)−C(6)	126.5(7)	C(5A)−N(1A)−C(7A)	114(2)	C(5A)−N(1A)−B(3)	122.5(14)
C(7A)−N(1A)−B(3)	123(2)	N(1A)−C(5A)−C(6A)	126(2)		

acid.[6] At the present time whether the initially formed intermediates in the synthesis of **2**−**6** involve the electrophile attaching itself to the iron center or to boron remains unresolved, although recent studies of other reactions of the compounds **1** suggest the latter. This is because electrophilic metal−ligand fragments can be coordinated by one or more BH vertexes without formation of metal−metal bonds.[1d] An interesting feature of the synthetic methodology employed here and previously[1c] is that starting from the reagent **1a**, it is possible to prepare complexes in which a donor molecule is either attached to the iron center or to the cage-boron atom, or bonded to both. In the latter instance the donor groups need not necessarily be the same as occurs in **3**−**6**. This provides a route to a variety of disparate ferracarboranes.

Reference was made earlier to the formation of **6**, where the weak donor $NCBu^t$ is attached to the cage. Very different results were obtained with acetonitrile as the base when using the hydride-abstracting reagents CF_3SO_3X (X = Me or H). Treatment of **1a** with NCMe in the presence of CF_3SO_3Me did not yield a product $[Fe(CO)_3(\eta^5\text{-}9\text{-}NCMe\text{-}7\text{-}CB_{10}H_{10})]$ akin to **6**. Instead the novel complex $[Fe(CO)_3(\eta^5\text{-}9\text{-}\{(E)\text{-}N(Me){=}C(H)Me\}\text{-}7\text{-}CB_{10}H_{10})]$ (**8**) was obtained. Similar products $[Fe(CO)_2(L)(\eta^5\text{-}9\text{-}\{(E)\text{-}N(Me){=}C(H)Me\}\text{-}7\text{-}CB_{10}H_{10})]$ (L = PPh_3 (**9**), $CNBu^t$ (**10**)) were obtained when **1b** and **1c**, respectively, were dissolved in NCMe and treated with CF_3SO_3Me. Data identifying these products are given in Tables 1−3, but their nature only became well established after X-ray diffraction studies had been carried out on compound **8.** Selected structural parameters are listed in Table 5, and the molecule is shown in Figure 2. Atom B(3), lying in a β-site in the $\overline{\mathrm{CB}BB\mathrm{B}}$ ring coordinated to the iron atom, carries an N(Me)= C(H)Me iminium substituent. Although the pendant iminium group was disordered with the N and =C atoms occupying two sites in an approximately 3:1 ratio, it was evident that the Me substituents had a transoid arrangement (B(3)−N = 1.562(6), C(5)−N = 1.301(10) Å, torsion angle C(7)−N−C(5)−C(6) = 175.0(8)° for the major component; B(3)−N(1A) = 1.67(2), C(5A)−N(1A) = 1.25(3) Å, torsion angle C(7A)−N(1A)−C(5A)−C(6A) = 168(2)° for the minor component). Comparison can be made with the structure of *endo*-9-N(H)=C(Me)Bu^t-*arachno*-6-SB_9H_{11} where an *arachno*-6-SB_9H_{11} cage bears an *endo*-oriented ketiminium substituent bound to a low-connectivity boron vertex.[7] Because of the *closo* nature of the ferracarborane moiety in **8**, the iminium substituent is strictly *exo*. The nitrogen atom in *endo*-9-N(H)=C(Me)Bu^t-*arachno*-6-SB_9H_{11}, however, acts as a two-electron donor, as it does in complex **8**, and the B−N bond length (1.542(5) Å) is correspondingly similar to that in **8**. The C=N iminium bond (1.284(4) Å) is also comparable in length with that observed in complex **8**, confirming that it lies within the double-bond range.

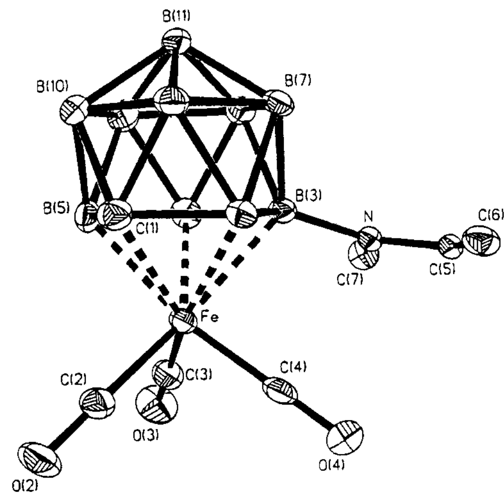

Figure 2. Structure of $[Fe(CO)_3(\eta^5\text{-}9\text{-}\{(E)\text{-}N(Me){=}C(H)Me\}\text{-}7\text{-}CB_{10}H_{10})]$ (**8**), showing the crystallographic labeling scheme. Hydrogen atoms are omitted for clarity, and thermal ellipsoids are shown at the 40% probability level.

A possible pathway for the formation of compounds **8**−**10** is shown in Scheme 1. It is proposed that in an initial step NCMe is methylated at the nitrogen atom by CF_3SO_3Me, giving the *N*-methylnitrilium cation $[MeN{\equiv}CMe]^+$. The formation of *N*-methylnitrilium salts from nitriles and methyl triflate is well established.[8] The cation $[MeN{\equiv}CMe]^+$ could then abstract H^- from a cage BH vertex to give an imine molecule. It is suggested that the tricarbonylferracarborane moiety should exert

(6) Quintana W.; Sneddon, L. G. *Inorg. Chem.* **1990**, *29*, 3242.

(7) Küpper, S.; Carroll, P. J.; Sneddon, L. G. *Inorg. Chem.* **1992**, *31*, 4921.

(8) (a) Alder, R. W.; Phillips, J. G. E. In *Encyclopedia of Reagents for Organic Synthesis*; Paquette, L. A., Ed.; Wiley: Chichester, 1995; Vol. 5, p 3617. (b) Booth, B. L.; Jibodu, K. O.; Proença, M. F. *J. Chem. Soc., Chem. Commun.* **1980**, 1151.

Scheme 1. Possible Mechanism of Formation of Complexes 8−10

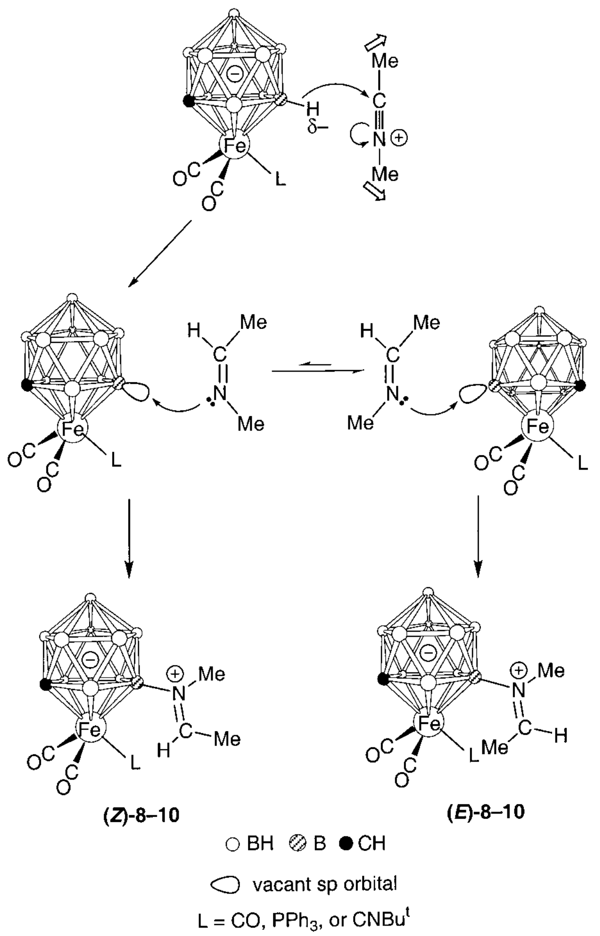

some regiochemical control over this process and necessarily yield the *Z*-isomer. The nitrogen atom of the imine so formed then coordinates to the vacant site created on the β-B vertex to give product **8**. As stated the Me groups are, however, trans in **8** and there was no evidence from NMR spectroscopy for the presence of any cis isomer in the crude product mixture. The *E*-forms of imines are more stable than the *Z*-configurations, and this must favor an evidently facile rearrangement of *Z*-N(Me)=C(H)Me into *E*-N(Me)=C(H)Me shown in Scheme 1, although geometric isomerization of the iminium group after it has been bound to the carborane cage cannot be ruled out.

The formation of compounds **8**−**10** instead of NCMe adducts $[Fe(CO)_2(L)(\eta^5\text{-}9\text{-NCMe-7-CB}_{10}H_{10})]$ is evidently due to the reagent CF_3SO_3Me reacting preferentially with NCMe rather than abstracting H^- from the cage. This is in contrast with the result when the reactants are **1b**, $NCBu^t$, and CF_3SO_3Me, since as described above, the complex $[Fe(CO)_2(PPh_3)(\eta^5\text{-}9\text{-NCBu}^t\text{-7-CB}_{10}H_{10})]$ (**6**) is formed. No isolable cage-substitution product was obtained by treating **1a** and $NCBu^t$ with CF_3SO_3Me. These results suggest that $NCBu^t$ is not as readily methylated as NCMe[8b] and that **1b** has a more hydridic β-BH site than **1a**.

Interestingly, no reaction occurred when mixtures of **1a** and NCMe were treated with CF_3SO_3H, there being no products formed akin to **6** or **8**. However, complex **1e** did react under these conditions, affording a mixture of $[Fe(CO)_2(PMe_2Ph)(\eta^5\text{-}9\text{-NCMe-7-CB}_{10}H_{10})]$ (**7**) and $[Fe(CO)_2(PMe_2Ph)(\eta^5\text{-}9\text{-}\{(E)\text{-N(H)=C(H)Me}\}\text{-7-CB}_{10}H_{10})]$ (**11**). Data characterizing these compounds are given in Tables 1−3. Evidently formation of **7** and **11** must proceed by two competing pathways. The replacement of a CO group in **1a** by PMe_2Ph to afford the precursor **1e** increases the electron density of the system, thus enhancing the hydridic nature of the cage-BH and thereby allowing in one pathway removal of H^- by H^+ and coordination of NCMe to give compound **7**. In the alternative pathway affording complex **11** the reagent CF_3SO_3H protonates NCMe to give $[HN{\equiv}CMe]^+$, which then reacts according to the steps in Scheme 1 to yield **11**. Since compounds **7** and **11** are formed in a ratio of about 1:2, protonation of NCMe is apparently the preferred route.

The presence in **11** of the (*E*)-N(H)=C(H)Me group is clearly revealed in the ^1H NMR spectrum (Table 2). Resonances for this moiety are seen in a 3:1:1 intensity ratio at δ 2.22 (d, Me, *J*(HH) 5 Hz), 7.84 (dq, =CH, *J*(HH) 5, 20 Hz), and 9.10 (d, NH, *J*(HH) 20 Hz). The *J*(HH) coupling of 20 Hz is diagnostic for the H atoms in a (*E*)-N(*H*)=C(*H*)Me configuration.[9] Other signals in the ^1H NMR spectrum are as expected. In the $^{13}C\{^1H\}$ NMR spectrum the asymmetry of the molecule results in two resonances (δ 214.3 and 212.4) for the nonequivalent CO groups, each a doublet due to $^{31}P-^{13}C$ coupling ($J(PC) = 29$ and 24 Hz, respectively). There is a signal at δ 176.1 for the C=N carbon and a broad peak at δ 47.5 for the cage CH group. A resonance at δ 5.8 in the $^{11}B\{^1H\}$ NMR spectrum (Table 3) remains a singlet in a fully coupled ^{11}B spectrum and can therefore be assigned to the boron atom bonded to the imine molecule.

Since the complexes **8**−**11** are, as far as we are aware, the first molecules known where an imine group is substituted on boron in a metallacarborane cage, investigation of some simple reactions was merited. The functionality of the imine group is relevant to general interest in derivatization of carborane frameworks.[10] Formally the β-boron-appended $[-N(Me){=}C(H)Me]^+$ group carries a positive charge. There are two canonical forms for the cationic fragment with the charge residing either on the N atom or on the C atom to which it is attached, the former naturally being favored. It would be anticipated therefore that the imine group would react with nucleophiles such as OH^- or H^- at the carbon center, and this was confirmed by experiment. Compound **8** in THF is hydrolyzed by traces of water to yield the complex $[Fe(CO)_3(\eta^5\text{-}9\text{-NH}_2\text{Me-7-CB}_{10}H_{10})]$ (**12**). This process is catalyzed by PMe_3 or amines, with the former giving a cleaner product. It is suggested that the reaction proceeds by the pathway shown in Scheme 2. Data for compound **12** (Tables 1−3) are in complete accord with its formulation.

The $[-N(Me){=}C(H)Me]^+$ group in **8** was also readily reduced by $[Na][BH_3CN]$, the reagent of choice for reducing imines and iminium salts.[11] The product obtained from **8** was the complex $[Fe(CO)_3(\eta^5\text{-}9\text{-}\{NH\text{-}$

(9) Jackman, L. M.; Sternhell, S. *Applications of Nuclear Magnetic Resonance Spectroscopy to Organic Chemistry*; Pergamon Press: Oxford, 1969.

(10) Grimes, R. N. *Coord. Chem. Rev.* **2000**, *200*−*202*, 773. Grimes, R. N. In *Contemporary Boron Chemistry;* Davidson, M., Hughes, A. K., Marder, T. B., Wade, K., Eds.; Royal Society of Chemistry: Cambridge, 2000; pp 283−290.

Table 6. Selected Internuclear Distances (Å) and Angles (deg) for [$Fe(CO)_3(\eta^5$-9-{NH(Me)Et}-7-$CB_{10}H_{10})$] (13)

Fe−C(4)	1.759(4)	Fe−C(2)	1.784(4)	Fe−C(3)	1.801(4)	Fe−C(1)	2.130(3)
Fe−B(5)	2.145(4)	Fe−B(2)	2.159(4)	Fe−B(3)	2.184(3)	Fe−B(4)	2.185(3)
B(3)−N	1.585(4)	C(2)−O(2)	1.138(4)	C(3)−O(3)	1.127(4)	C(4)−O(4)	1.140(4)
N−C(5)	1.474(4)	N−C(7)	1.487(4)	N−H(1a)	0.86		

C(4)−Fe−C(2)	94.3(2)	C(4)−Fe−C(3)	89.5(2)	C(2)−Fe−C(3)	91.2(2)
C(4)−Fe−C(1)	159.92(14)	C(2)−Fe−C(1)	105.7(2)	C(3)−Fe−C(1)	91.73(14)
C(4)−Fe−B(5)	113.0(2)	C(2)−Fe−B(5)	151.7(2)	C(3)−Fe−B(5)	82.0(2)
C(4)−Fe−B(2)	138.3(2)	C(2)−Fe−B(2)	80.6(2)	C(3)−Fe−B(2)	131.7(2)
C(4)−Fe−B(3)	92.90(14)	C(2)−Fe−B(3)	103.2(2)	C(3)−Fe−B(3)	165.2(2)
C(4)−Fe−B(4)	79.91(14)	C(2)−Fe−B(4)	150.7(2)	C(3)−Fe−B(4)	117.3(2)
N−B(3)−B(8)	113.2(2)	N−B(3)−B(7)	111.2(3)	N−B(3)−B(2)	123.7(3)
N−B(3)−B(4)	126.1(3)	N−B(3)−Fe	121.2(2)	O(2)−C(2)−Fe	178.8(4)
O(3)−C(3)−Fe	178.3(3)	O(4)−C(4)−Fe	178.5(3)	C(5)−N−C(7)	113.4(3)
C(5)−N−B(3)	115.8(2)	C(7)−N−B(3)	115.7(3)	N−C(5)−C(6)	115.5(3)
H(1a)−N−C(5)	98	H(1a)−N−C(7)	104	H(1a)−N−B(3)	107

Scheme 2. PMe_3-Catalyzed Hydrolysis of Complex 8

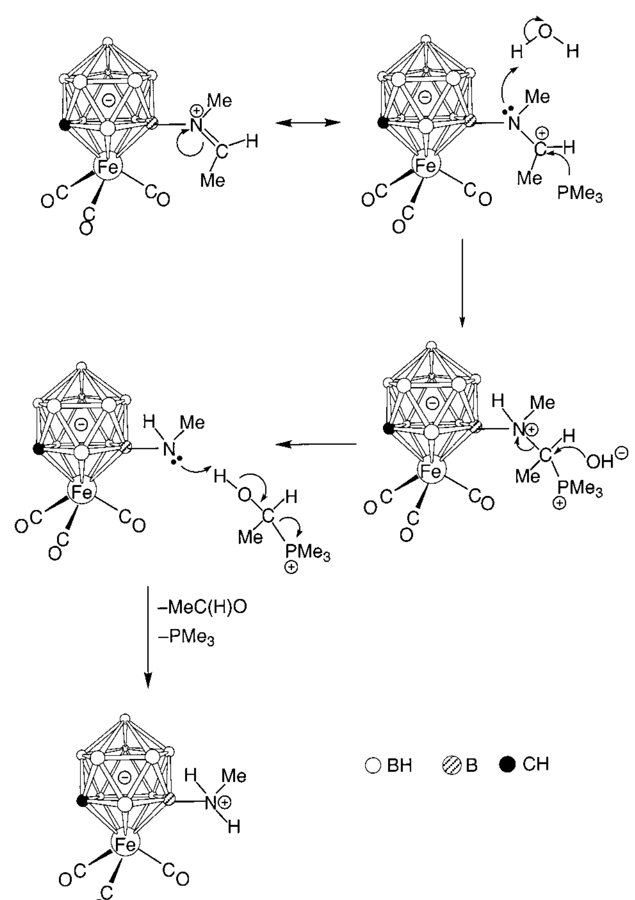

(Me)Et}-7-$CB_{10}H_{10})$] (**13**), the nature of which was established by a single-crystal X-ray diffraction study. The molecule is shown in Figure 3, and selected structural parameters are listed in Table 6. The presence of the NH(Me)Et group attached to a β-boron atom in the pentagonal CB*BB*B ring ligating the iron is clearly evident (B(3)−N = 1.585(4) Å). Atom H(1A) was located in a difference Fourier synthesis. The N atom is a chiral center which, coupled with the planar chirality imposed by substitution at one of the β-B vertexes in the CB*BB*B ring, gives rise to two diastereomeric pairs of enantiomers. Additonally the methylene protons of the NEt group are diastereotopic. Thus peaks for the NH(Me)(Et) fragment are duplicated, giving theoretically two resonances for the NMe protons and four for the methylene protons. Alas due to some overlap of poorly resolved signals, not all are fully identified with multiplets at δ 2.66, 2.76, 3.35, and 3.48 for all these protons. The signals due to the CH_2*Me* (δ 1.30) and NH (3.97) protons are also broad but clearly integrate to six and two hydrogens, respectively. Furthermore, the broad resonance resulting from the cage CH group also accounts for two protons by integration. The $^{13}C\{^1H\}$ NMR spectrum is less cluttered, with two resonances each for the CH_2Me (δ 52.7 and 52.5), NMe (40.5 and 40.3), and CH_2*Me* (12.7 and 12.6) groups. The transmittance of the effects of this diastereomeric asymmetry to the cage CH proton is less evident, with one signal observed at δ 48.9, albeit broad, and even less so to the $Fe(CO)_3$ groups, with just one resonance at δ 207.1. The $^{11}B\{^1H\}$ NMR spectrum (Table 3) shows a resonance at δ 12.6, which remained a singlet in a fully coupled ^{11}B spectrum, a feature diagnostic for a cage boron carrying an exopolyhedral substituent other than hydrogen.

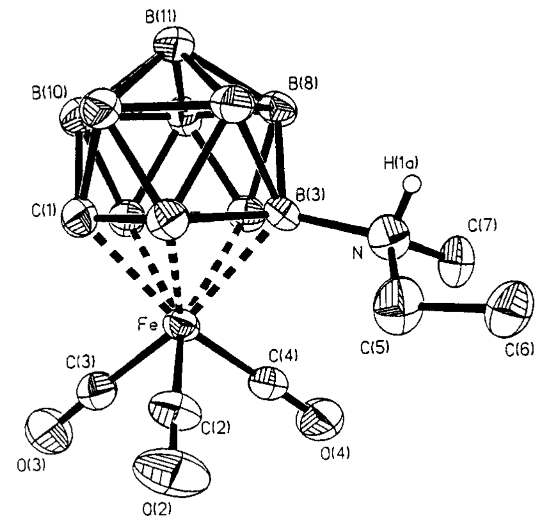

Figure 3. Structure of [$Fe(CO)_3(\eta^5$-9-{NH(Me)Et}-7-$CB_{10}H_{10})$] (**13**), showing the crystallographic labeling scheme. Except for H(1a), hydrogen atoms are omitted for clarity, and thermal ellipsoids are shown at the 40% probability level.

We have previously shown that reactions between the ruthenacarborane [$Ru(CO)_2(THF)(\eta^5$-7,8-$C_2B_9H_{11})$] and

(11) Hutchins R. O. In *Comprehensive Organic Synthesis*; Trost, B. M., Fleming, I., Eds.; Pergamon (Elsevier): Oxford, 1991; Vol. 8, Section 1.2.

alkynes RC≡CH result in insertion of the organic moiety into a cage BH to yield products containing α- or *β*-B−(*E*)-C(H)=C(H)R groups.[12] The likely pathway for the process involves initial displacement of THF from the precursor to give a Ru(η^2-RC≡CH) complex, which rearranges into Ru=C=C(H)R. The vinylidene moiety then inserts into a BH bond. It was of interest therefore to determine if **1a** would react in a similar manner with an alkyne of the type RC≡CH.

Treatment of **1a** in THF with Bu^{t}C≡CH, in the presence of Me_3NO, which was added to facilitate removal of a CO molecule, afforded a product formulated as [N($PPh_3)_2$][Fe$(CO)_2$(η^2:η^5-*n*-{(*E*)-C(H)=C(H)Bu^t}-7-$CB_{10}H_{10}$)] (**14**, with *n* = 8 or 9), a species closely related to the neutral dicarbollide ruthenium compound [Ru-$(CO)_2$(η^2:η^5-*n*-{(*E*)-C(H)=C(H)Bu^t}-7,8-$C_2B_9H_{10}$)] (isomers, *n* = 9 and 10).[12] Careful examination of the NMR spectra of the salt **14** revealed that only one isomer was formed, but the data did not permit a distinction to be made between attachment of the (*E*)-C(H)=C(H)Bu^t group to a B atom in an α (*n* = 8) site and attachment in a *β* (*n* = 9) site with respect to the carbon in the metal-coordinated CBBBB ring. Moreover, compound **14** was invariably formed contaminated with the salts [N($PPh_3)_2$][*closo*-2-$CB_{10}H_{11}$] and [N($PPh_3)_2$][*nido*-7-$CB_{10}H_{13}$]. Repeated chromatography of the mixture failed to yield a satisfactory microanalytical sample. However, a mass spectrum showed the molecular ion [**14**]$^+$ (Table 1), and NMR data (Tables 2 and 3) established the presence of a B−C(H)=C(H)Bu^t group (^{11}B{^{1}H} NMR spectrum: *δ* 12.6). The ^{1}H−^{1}H coupling constant (*J*(HH) = 11 Hz) for the alkenyl protons B−C(*H*)=C(*H*)Bu^t in the ^{1}H NMR spectrum is somewhat smaller than that expected for a trans configuration and almost suggestive of a cis arrangement of this fragment. These isomers had not been previously observed in the ruthenacarborane work,[12] and clearly firmer structural verification was required.

A derivative of complex **14** was prepared by reaction with PPh_3. The product obtained, [N($PPh_3)_2$][Fe$(CO)_2$-(PPh_3)(η^5-*n*-{(*E*)-C(H)=C(H)Bu^t}-7-$CB_{10}H_{10}$)] (**15**), could be isolated pure and was characterized by microanalysis and by its NMR spectra (Tables 1−3), although again the site of attachment (*n* = 8 or 9) of the B−C(H)=C(H)-Bu^t group to the cage system was unresolved. The ^{1}H NMR spectral data were, however, more conclusive with regard to the configuration of the η^2-alkenyl group. With a ^{1}H−^{1}H coupling constant for the B−C(*H*)=C(*H*)Bu^t protons *J*(HH) = 18 Hz, the trans arrangement would seem to be confirmed, as geometric isomerization during the reaction with PPh_3 is extremely unlikely. Conversion of **14** into **15** occurs with a lifting of the η^2 coordination of the B−(*E*)-C(H)=C(H)Bu^t moiety to the iron, a reaction step previously observed in reactions with dicarbollide ruthenium species.[12]

The site of attachment of the (*E*)-C(H)=C(H)Bu^t group to the cage system in **14** and **15** was resolved by a single-crystal X-ray diffraction study on the molecule [Fe$(CO)_2$-(η^2:η^5-8-{(*E*)-C(H)=C(H)Bu^t}-10-{(*E*)-N(Me)=C(H)Me}-7-$CB_{10}H_9$)] (**16**). This complex was prepared by treating compound **14** in NCMe with CF_3SO_3Me. The structure

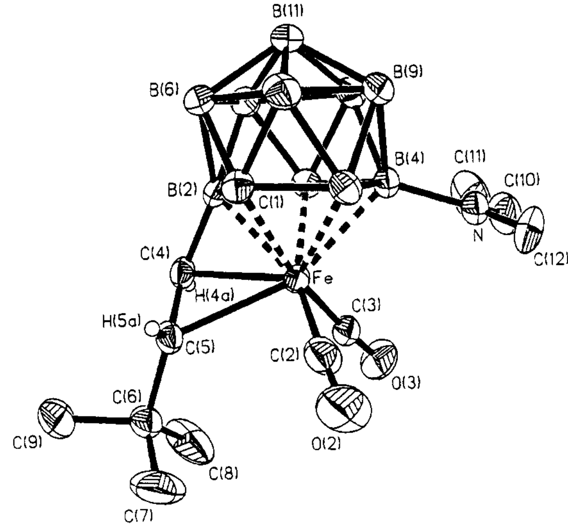

Figure 4. Structure of [Fe$(CO)_2$(η^2:η^5-8-{(*E*)-C(H)=C(H)-Bu^t}-10-{(*E*)-N(Me)=C(H)Me}-7-$CB_{10}H_9$)] (**16**), showing the crystallographic labeling scheme. Except for H(5a) and H(4a), hydrogen atoms are omitted for clarity, and thermal ellipsoids are shown at the 40% probability level.

Chart 2

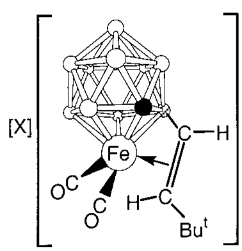

14

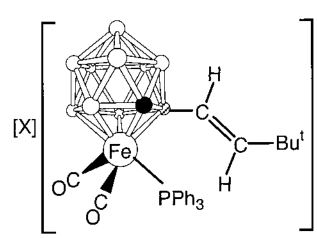

15

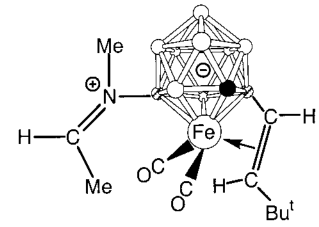

16

[X] = [N($PPh_3)_2$]

○ BH ◍ B ● CH

is shown in Figure 4, and selected bond distances and angles are given in Table 7. The (*E*)-C(H)=C(H)Bu^t group is bonded to an α-boron vertex (B(2)−C(4) = 1.527(5) Å), from which it may reasonably be inferred that it is also bonded in this manner in complexes **14** and **15**. The trans arrangements of both the η^2-alkenyl (torsion angle B(2)−C(4)−C(5)−C(6) 171.9(3)°) and the iminium (torsion angle C(11)−C(10)−N−C(12) 178.6(6)°) fragments are confirmed. The alkenyl hydrogen atoms H(4a) and H(5a) were located from difference Fourier syntheses and displayed a 14 Hz ^{1}H−^{1}H coupling in the ^{1}H NMR spectrum (Table 2), which is within the limits for *trans*-alkenyl protons.[9] The η^2 ligation of the iron by the double bond of the vinyl group (C(4)−C(5) = 1.386(5) Å, Fe−C(4) = 2.129(3) Å, Fe−C(5) = 2.289(3) Å) is similar to that found by X-ray diffraction

(12) Anderson, S.; Mullica, D. F.; Sappenfield, E. L.; Stone, F. G. A. *Organometallics* **1996**, *15*, 1676.

Table 7. Selected Internuclear Distances (Å) and Angles (deg) for [Fe(CO)$_2$(η^2: η^5-8-{(*E*)-C(H)═C(H)Bu^t}-10-{(*E*)-N(Me)═C(H)Me}-7-CB$_{10}$H$_9$)] (16)

Fe−C(3)	1.753(4)	Fe−C(2)	1.776(4)	Fe−B(2)	2.034(4)	Fe−C(1)	2.121(3)
Fe−C(4)	2.129(3)	Fe−B(5)	2.148(4)	Fe−B(4)	2.181(4)	Fe−B(3)	2.190(3)
Fe−C(5)	2.289(3)	B(2)−C(4)	1.527(5)	B(4)−N	1.559(5)	C(2)−O(2)	1.149(5)
C(3)−O(3)	1.144(4)	C(4)−H(4A)	0.96	C(4)−C(5)	1.386(5)	C(5)−H(5A)	0.91
N−C(10)	1.278(6)	N−C(12)	1.467(6)				

C(3)−Fe−C(2)	91.7(2)	C(3)−Fe−B(2)	122.8(2)	C(2)−Fe−B(2)	142.1(2)
C(3)−Fe−C(1)	167.3(2)	C(2)−Fe−C(1)	99.6(2)	C(3)−Fe−C(4)	100.1(2)
C(2)−Fe−C(4)	122.7(2)	B(2)−Fe−C(4)	43.0(2)	C(1)−Fe−C(4)	78.81(14)
C(3)−Fe−B(5)	129.7(2)	C(2)−Fe−B(5)	84.4(2)	C(4)−Fe−B(5)	123.9(2)
C(3)−Fe−B(4)	88.7(2)	C(2)−Fe−B(4)	113.8(2)	C(4)−Fe−B(4)	122.3(2)
C(3)−Fe−B(3)	83.9(2)	C(2)−Fe−B(3)	161.5(2)	C(4)−Fe−B(3)	75.82(14)
C(3)−Fe−C(5)	103.3(2)	C(2)−Fe−C(5)	86.4(2)	B(2)−Fe−C(5)	71.73(14)
C(1)−Fe−C(5)	83.50(14)	C(4)−Fe−C(5)	36.27(13)	B(5)−Fe−C(5)	126.4(2)
B(4)−Fe−C(5)	156.48(14)	B(3)−Fe−C(5)	112.09(14)	C(4)−B(2)−Fe	71.8(2)
N−B(4)−B(3)	127.2(3)	N−B(4)−B(5)	119.5(3)	N−B(4)−Fe	117.2(3)
O(2)−C(2)−Fe	177.9(4)	O(3)−C(3)−Fe	176.4(4)	C(5)−C(4)−B(2)	121.6(4)
H(4A)−C(4)−C(5)	117	H(4A)−C(4)−B(2)	118	H(4A)−C(4)−Fe	111
H(5A)−C(5)−C(4)	119	H(5A)−C(5)−C(6)	112	H(5A)−C(5)−Fe	97
C(5)−C(4)−Fe	78.2(2)	B(2)−C(4)−Fe	65.2(2)	C(4)−C(5)−C(6)	124.9(4)
C(4)−C(5)−Fe	65.6(2)	C(6)−C(5)−Fe	128.5(3)	C(10)−N−C(12)	116.6(4)
C(10)−N−B(4)	128.2(4)	C(12)−N−B(4)	115.2(3)	N−C(10)−C(11)	128.8(5)

with the dicarbollide ruthenium species [Ru(CO)$_2$(η^2:η^5-9-{(*E*)-C(H)═C(H)Bu^t}-7,8-C$_2$B$_9$H$_{10}$)].[12]

Conclusions

The substituent on the cage in the charge-compensated complexes **2**−**6** formally reduces the charge on the [*nido*-7-CB$_{10}$H$_{11}$]$^{3-}$ ligands present in their precursors from −3 to −2. This allows the design of new ferracarborane reagents of Fe^{II} for further syntheses and the preparation of new complexes with different combinations of functional groups ligating the iron. The synthesis of the iminium derivatives **8**−**11** using the reagents CF$_3$SO$_3$X (X = Me or H) makes possible further derivatization of the cage system by reactions at the iminium group. There is a definite trend in these substitutions for attack and replacement of a β-B−H bond in the CB*BB*B ring. The reactions result from a direct hydride abstraction by X$^+$ from CF$_3$SO$_3$X, and the cause may be due to a subtle increase in polarity of the β-B$^{\delta+}$−H$^{\delta-}$ bonds over the adjacent α-B$^{\delta+}$−H$^{\delta-}$ bonds. However, when the substitution reaction proceeds via a vinylidene insertion of a ═C═C(H)Bu^t group (i.e., hydroboration, as in the formation of complex **14**), α-B−H bonds in the C*B*BB*B* ring are apparently favored. Thus the mechanism of hydroboration may be less dependent on the polarity of the B−H bonds. The products formed from the hydride abstraction may therefore be more kinetically controlled, while the distribution for hydroboration is more dependent on the frontier orbital energies; that is, control is thermodynamic.

Experimental Section

General Considerations. All reactions were carried out under an atmosphere of dry nitrogen using Schlenk line techniques. Solvents were distilled from appropriate drying agents under nitrogen prior to use. Petroleum ether refers to that fraction of boiling point 40−60 °C. Chromatography columns (ca. 15 cm in length and ca. 2 cm in diameter) were packed with silica gel (Acros, 60−200 mesh). NMR spectra were recorded at the following frequencies: ^{1}H 360.13, ^{13}C 90.56, ^{31}P 145.78, and ^{11}B 115.5 MHz. The salt [NHMe$_3$][*nido*-7-CB$_{10}$H$_{13}$] was synthesized from 7-NMe$_3$-*nido*-7-CB$_{10}$H$_{12}$ according to the method of Knoth et al.[13] The complex [N(PPh$_3$)$_2$][Fe(CO)$_3$(η^5-7-CB$_{10}$H$_{11}$)] was prepared according to literature methods.[1c]

Synthesis of [N(PPh$_3$)$_2$][Fe(CO)$_2$(L)(η^5-7-CB$_{10}$H$_{11}$)] (L = SMe$_2$, PMe$_2$Ph). (i) Compound **1a** (0.40 g, 0.50 mmol) was dissolved in SMe$_2$ (10 mL), and Me$_3$NO (0.15 g, 2.00 mmol) was added. The mixture was stirred for 24 h, solvent removed in vacuo, and the residue treated with CH$_2$Cl$_2$ (15 mL). After filtration through a Celite plug, ca. 2 g of silica gel was added to the filtrate. Solvent was removed in vacuo, affording a yellow brownish powder, which was transferred to the top of a chromatography column. Elution with pure CH$_2$Cl$_2$ gave a yellow fraction. Removal of solvent in vacuo yielded yellow microcrystals of [N(PPh$_3$)$_2$][Fe(CO)$_2$(SMe$_2$)(η^5-7-CB$_{10}$H$_{11}$)] (**1d**) (0.34 g).

(ii) The compound [N(PPh$_3$)$_2$][Fe(CO)$_2$(PMe$_2$Ph)(η^5-7-CB$_{10}$H$_{11}$)] (**1e**) (0.33 g) was similarly obtained from **1a** (0.40 g, 0.50 mmol) and PMe$_2$Ph (0.35 g, 5.00 mmol).

Synthesis of [Fe(CO)$_2$(SMe$_2$)(η^5-9-L′-7-CB$_{10}$H$_{10}$)] (L′ = SMe$_2$, O(CH$_2$)$_4$). (i) Compound **1d** (0.42 g, 0.50 mmol) was dissolved in SMe$_2$ (20 mL) and concentrated H$_2$SO$_4$ (0.50 mL) added. After stirring for 24 h solvent was removed in vacuo, and the residue treated with CH$_2$Cl$_2$ (15 mL). After filtration through a Celite plug, ca. 2 g of silica gel was added to the filtrate. Solvent was removed in vacuo affording a yellow powder, which was transferred to the top of a chromatography column. Elution with a mixture of CH$_2$Cl$_2$−petroleum ether (3:2) gave a yellow fraction. Removal of solvent in vacuo gave yellow microcrystals of [Fe(CO)$_2$(SMe$_2$)(η^5-9-SMe$_2$-7-CB$_{10}$H$_{10}$)] (**2**) (0.10 g).

(ii) Compound **1d** (0.42 g, 0.50 mmol) in THF (20 mL) was stirred with concentrated H$_2$SO$_4$ (0.50 mL) for 24 h. The remaining THF was removed in vacuo, and the residue (polymerized THF and product) was treated with CH$_2$Cl$_2$ (15 mL). After filtration through a Celite plug and removal of solvent yellow microcrystals of [Fe(CO)$_2$(SMe$_2$)(η^5-9-O(CH$_2$)$_4$-7-CB$_{10}$H$_{10}$)] (**3**) (0.15 g) were obtained.

Synthesis of [Fe(CO)$_2$(PPh$_3$)(η^5-9-L′-7-CB$_{10}$H$_{10}$)] (L = SMe$_2$, O(CH$_2$)$_4$ and NCBu^t). (i) Compound **1b** (0.53 g, 0.50 mmol) was dissolved in CH$_2$Cl$_2$−SMe$_2$ (20 mL, 1:1), and CF$_3$SO$_3$H (0.25 mL) was added. After stirring (24 h), solvent was removed in vacuo and the residue treated with CH$_2$Cl$_2$ (15 mL). After filtration through a Celite plug, ca. 2 g of silica gel was added to the filtrate. Solvent was removed in vacuo, affording

(13) Knoth, W. H.; Little, J. L.; Lawrence, J. R.; Todd, L. J. *Inorg. Synth.* **1968**, *11*, 33.

Table 8. Data for X-ray Crystal Structure Analyses

	2	8	13	16
cryst dimens (mm)	0.54 × 0.13 × 0.10	0.52 × 0.49 × 0.24	0.36 × 0.30 × 0.20	0.70 × 0.36 × 0.29
formula	$C_7H_{22}B_{10}FeO_2S_2$	$C_7H_{17}B_{10}FeNO_3$	$C_7H_{19}B_{10}FeNO_3$	$C_{12}H_{27}B_{10}FeNO_2$
M_r	366.32	327.17	329.18	381.30
cryst color, shape	amber needles	yellow prisms	pale-yellow prisms	orange blocks
cryst syst	orthorhombic	monoclinic	monoclinic	orthorhombic
space group	$P2_12_12_1$	$P2_1/c$	$P2_1/c$	$P2_12_12_1$
a (Å)	6.7065(14)	13.2967(13)	12.325(2)	9.3727(13)
b (Å)	14.0124(11)	8.978(3)	7.6538(10)	12.8796(8)
c (Å)	18.680(2)	13.820(3)	17.502(2)	16.719(2)
β (deg)		109.755(11)	106.856(14)	
V (Å^3)	1755	1553	1580	2018
Z	4	4	4	4
d_{calcd} (g cm^{-3})	1.386	1.400	1.384	1.255
μ(Mo Kα) (cm^{-1})	10.89	9.70	9.53	7.52
F(000) (e)	752	664	672	792
T (K)	183(2)	183(2)	293(2)	293(2)
2θ range (deg)	3.6−50.0	3.2−50.0	3.4−45.0	4.0−50.0
no. of reflns coll (excld stds)	3478	2795	2171	2166
no. of unique reflns	3071	2671	2059	2140
no. of obsd reflns	2741	2437	1771	1998
refln limits: h, k, l	0 to 7; 0 to 16; −22 to 22	0 to 15; 0 to 10; −16 to 15	0 to 13; 0 to 8; −18 to 18	0 to 11; 0 to 15; −1 to 19
no. of params refined	200	236	202	245
final residuals wR_2 (R_1) all data[a]	0.0720 (0.0330)[b]	0.0936 (0.0399)	0.0838 (0.0335)	0.0817 (0.0311)[c]
weighting factors[a]	a = 0.0324, b = 0.3544	a = 0.0336, b = 1.0333	a = 0.0398, b = 1.4400	a = 0.0454, b = 0.9491
goodness of fit on F^2	1.040	1.207	1.038	1.056
final electron density diff features (max/min)/e Å^{-3}	0.232, −0.216	0.352, −0.264	0.336, −0.324	0.293, −0.408

[a] Refinement was block full-matrix least-squares on all F^2 data: $wR_2 = [\sum\{w(F_o^2 - F_c^2)^2\}/\sum w(F_o^2)^2]^{1/2}$ where $w^{-1} = [\sigma^2(F_o^2) + (aP)^2 + bP]$ where $P = [\max(F_o^2,0) + 2F_c^2]/3$. The value in parentheses is given for comparison with refinements based on F_o with a typical threshold of $F_o > 4\sigma(F_o)$ and $R_1 = \sum||F_o| - |F_c||/\sum|F_o|$ and $w^{-1} = [\sigma^2(F_o) + g(F_o^2)]$. [b] Flack parameter = 0.47(2). [c] Flack parameter = 0.03(3).

a yellow powder, which was transferred to the top of a chromatography column. Elution with CH_2Cl_2−petroleum ether (3:2) afforded a pale yellow fraction. Removal of solvent in vacuo gave pale yellow microcrystals of [Fe(CO)$_2$(PPh$_3$)(η^5-9-SMe$_2$-7-CB$_{10}$H$_{10}$)] (**4**) (0.22 g).

(ii) Similarly **1b** (0.53 g, 0.50 mmol) in CH_2Cl_2−THF (20 mL, 1:1) with CF_3SO_3H (0.25 mL) yielded pale yellow microcrystals of [Fe(CO)$_2$(PPh$_3$)(η^5-9-O(CH$_2$)$_4$-7-CB$_{10}$H$_{10}$)] (**5**) (0.23 g).

(iii) Compound **1b** (0.53 g, 0.50 mmol) in CH_2Cl_2−NCBu^t (10 mL, 4:1) with CF_3SO_3Me (0.25 mL) yielded pale yellow microcrystals of [Fe(CO)$_2$(PPh$_3$)(η^5-9-NCBu^t-7-CB$_{10}$H$_{10}$)] (**6**) (0.18 g).

Synthesis of [Fe(CO)$_2$(PMe$_2$Ph)(η^5-9-L′-7-CB$_{10}$H$_{10}$)] (L′ = NCMe, (*E*)-N(H)=C(H)Me). Compound **1e** (0.46 g, 0.50 mmol) was dissolved in NCMe (10 mL), and CF_3SO_3H (0.25 mL) was added. After stirring for 24 h, solvent was removed in vacuo, and the residue was taken up in CH_2Cl_2 (15 mL). After filtration through a Celite plug, ca. 2 g of silica gel was added to the filtrate. Solvent was removed in vacuo, affording a yellow powder, which was transferred to the top of a chromatography column. Elution with a mixture of CH_2Cl_2−petroleum ether (4:1) gave a pale yellow fraction. Removal of solvent in vacuo yielded pale yellow microcrystals of [Fe(CO)$_2$(PMe$_2$Ph)(η^5-9-NCMe-7-CB$_{10}$H$_{10}$)] (**7**) (0.05 g). Further elution with neat CH_2Cl_2 removed a yellow fraction. Removal of solvent in vacuo yielded yellow microcrystals of [Fe(CO)$_2$(PMe$_2$Ph)(η^5-9-{(*E*)-N(H)=C(H)Me}-7-CB$_{10}$H$_{10}$)] (**11**) (0.09 g).

Synthesis of [Fe(CO)$_2$(L)(η^5-9-{(*E*)-N(Me)=C(H)Me}-7-CB$_{10}$H$_{10}$)] (L = CO, CNBu^t, PPh$_3$). (i) Compound **1a** (0.40 g, 0.50 mmol) was dissolved in NCMe (10 mL), and CF_3SO_3Me (0.25 mL) was added. Using a procedure similar to that which gave **11**, but eluting the chromatography column with CH_2Cl_2−petroleum ether (3:2), afforded pale yellow microcrystals of [Fe(CO)$_3$(η^5-9-{(*E*)-N(Me)=C(H)Me}-7-CB$_{10}$H$_{10}$)] (**8**) (0.07 g).

(ii) Compound **1b** (0.53 g, 0.50 mmol) in CH_2Cl_2−NCMe (20 mL, 1:1) with CF_3SO_3Me (0.25 mL) similarly yielded pale yellow microcrystals of [Fe(CO)$_2$(PPh$_3$)(η^5-9-{(*E*)-N(Me)=C(H)-Me}-7-CB$_{10}$H$_{10}$)] (**9**) (0.24 g).

(iii) Similarly compound **1c** (0.43 g, 0.50 mmol) in NCMe (10 mL) with CF_3SO_3Me (0.25 mL) yielded pale yellow microcrystals of [Fe(CO)$_2$(CNBu^t)(η^5-9-{(*E*)-N(Me)=C(H)Me}-7-CB$_{10}$H$_{10}$)] (**10**) (0.16 g).

Reactions of [Fe(CO)$_3$(η^5-9-{(*E*)-N(Me)=C(H)Me}-7-CB$_{10}$H$_{10}$)] (8). (i) Compound **8** (0.16 g, 0.50 mmol) was dissolved in THF (10 mL), and a PMe$_3$ solution in THF (1.0 M, 2 mL) was added. After stirring for 24 h the solvent was removed in vacuo, and the residue taken up in CH_2Cl_2 (15 mL). Following filtration through a Celite plug, ca. 2 g of silica gel was added to the filtrate. Solvent was removed in vacuo, affording a yellow powder, which was transferred to a chromatography column. Elution with a mixture of CH_2Cl_2−NCMe (24:1) gave a pale yellow fraction. Removal of solvent in vacuo yielded pale yellow microcrystals of [Fe(CO)$_3$(η^5-9-NH$_2$Me-7-CB$_{10}$H$_{10}$)] (**12**) (0.13 g).

(ii) Similarly, compound **8** (0.16 g, 0.50 mmol) with [Na][BH$_3$CN] (0.06 g, 0.63 mmol) in MeOH (10 mL) yielded pale yellow microcrystals of [Fe(CO)$_3$(η^5-9-{NH(Me)Et}-7-CB$_{10}$H$_{10}$)] (**13**) (0.14 g) following chromatographic purification eluting with neat CH_2Cl_2.

Synthesis of [N(PPh$_3$)$_2$][Fe(CO)$_2$(η^2:η^5-8-{(*E*)-C(H)=C(H)Bu^t}-7-CB$_{10}$H$_{10}$)]. A sample of **1a** (0.40 g, 0.50 mmol) was dissolved in THF (10 mL), and Bu^{t}C≡CH (0.5 mL) and Me$_3$NO (0.15 g, 2 mmol) were added and the mixture was stirred for 24 h. Using a workup method similar to that which gave compound **12**, but eluting the chromatography column with neat CH_2Cl_2, gave deep yellow microcrystals of [N(PPh$_3$)$_2$][Fe(CO)$_2$(η^2:η^5-8-{(*E*)-C(H)=C(H)Bu^t}-7-CB$_{10}$H$_{10}$)] (**14**) (0.19 g). The product is always contaminated with the salts [N(PPh$_3$)$_2$][*closo*-2-CB$_{10}$H$_{11}$] (0.17 g, 51%) and [N(PPh$_3$)$_2$][*nido*-7-CB$_{10}$H$_{13}$] (0.01 g, 4%). The yield calculation is based on the relative peak integrals in the NMR spectra.

Synthesis of [N(PPh$_3$)$_2$][Fe(CO)$_2$(PPh$_3$)(η^5-8-{(*E*)-C(H)=C(H)Bu^t}-7-CB$_{10}$H$_{10}$)]. Compound **14** (0.43 g of the crude material) was dissolved in THF (10 mL), and PPh_3 (0.52 g, 2.00 mmol) was added. After stirring for 24 h, the solvent was removed in vacuo, and the residue was treated with CH_2Cl_2 (15 mL). Following filtration through a Celite plug, ca. 2 g of silica gel was added to the filtrate. Solvent was removed in vacuo, affording a yellow powder, which was transferred to a chromatography column (15 cm). Elution with a neat CH_2Cl_2 and removal of solvent in vacuo yielded yellow microcrystals of $[N(PPh_3)_2][Fe(CO)_2(PPh_3)(\eta^5\text{-}8\text{-}\{(E)\text{-}C(H){=}C(H)Bu^t\}\text{-}7\text{-}CB_{10}H_{10})]$ (**15**) (0.25 g).

Synthesis of $[Fe(CO)_2(\eta^2{:}\eta^5\text{-}8\text{-}\{(E)\text{-}C(H){=}C(H)Bu^t\}\text{-}10\text{-}\{(E)\text{-}N(Me){=}C(H)Me\}\text{-}7\text{-}CB_{10}H_9)]$. Using the same procedure as that described for the synthesis of **8**, compound **14** (0.22 g, 0.25 mmol) in NCMe (10 mL) with CF_3SO_3Me (0.25 mL) yielded deep yellow microcrystals of $[Fe(CO)_2(\eta^2{:}\eta^5\text{-}8\text{-}\{(E)\text{-}C(H){=}C(H)Bu^t\}\text{-}10\text{-}\{(E)\text{-}N(Me){=}C(H)Me\}\text{-}7\text{-}CB_{10}H_9)]$ (**16**) (0.04 g).

Crystal Structure Determinations and Refinements. Experimental data for **2**, **8**, **13**, and **16** are shown in Table 8. Diffracted intensities were collected on an Enraf-Nonius CAD-4 diffractometer using graphite-monochromated Mo Kα X-radiation operating in the ω-1/3θ (**13**), ω-2/3θ (**8**), ω-4/3θ (**16**), and ω-5/3θ (**2**) scan modes. Final unit cell dimensions were determined from the setting angles of 25 accurately centered reflections. Crystal stability during the data collection was monitored by measuring the intensities of three standard reflections every 2 h. Low-temperature data (183 K) were collected at a varied rate of 4.13−5.17 deg min^{-1} in ω with a scan range of $1.05 + 0.34 \tan\theta$ for **2** and a constant speed of 5.17 deg min^{-1} in ω with a scan range of $1.40 + 0.34 \tan\theta$ for **8**. Room-temperature data were collected at a constant speed of 5.17 deg min^{-1} in ω with a scan range of $1.25 + 0.34 \tan\theta$ for **13** and **16**. The data were corrected for Lorentz, polarization, and X-ray absorption effects, the last using a numerical method based on the measurements of crystal faces.

The structures were solved by direct methods, and successive difference Fourier syntheses were used to locate all non-hydrogen atoms using SHELXTL version 5.03.[14] Refinements were made by full-matrix least-squares on all F^2 data using SHELXL-97.[15] Anisotropic thermal parameters were included for all non-hydrogen atoms. For all structures, cage carbon atoms were assigned by comparison of the bond lengths to adjacent boron atoms in conjunction with the magnitudes of their isotropic thermal parameters. With the exception of H(1a) in **13** along with H(4), H(5a), and H(10a) in **16**, all hydrogen atoms were included in calculated positions and allowed to ride on their parent boron or carbon atoms with fixed isotropic thermal parameters ($U_{iso} = 1.2U_{iso}$ of the parent atom or $U_{iso} = 1.5U_{iso}$ for methyl protons). The remaining hydrogens, H(1a) in **13** and H(4a), H(5a), and H(10a) in **16**, were located in difference Fourier syntheses. The positional parameters of these hydrogens were allowed to refine while their isotropic thermal parameters were constrained to $1.2U_{iso}$ of the parent nitrogen or carbon atoms. The pendant iminium group in compound **8** was disordered over two distinct sites in 73:27 and 52:48% ratios, respectively. The absolute configurations of compounds **2** and **16** were determined by examination of the appropriate Flack parameters (Table 8, footnotes *b* and *c*).[16] All calculations were carried out on Dell PC computers.

Acknowledgment. We thank Professor Roger Alder for helpful discussions in connection with the work involving nitriles and the Robert A. Welch Foundation for support (Grant AA-1201).

Supporting Information Available: Tables of atomic coordinates and *U* values, bond lengths and angles, and anisotropic thermal parameters and ORTEP diagrams for **2**, **8**, **13**, and **16** in CIF format. This material is available free of charge via the Internet at http://pubs.acs.org.

OM001057X

(14) *SHELXTL* version 5.03, Bruker AXS: Madison, WI, 1995.
(15) Sheldrick, G. M. *SHELXL-97*; University of Göttingen: Göttingen, Germany, 1997.
(16) Flack, H. D. *Acta Crystallogr.* **1983**, *A39*, 876.